Photoconductivity study of synthetic FeS_2 single crystals at low temperatures

1994 J. Phys.: Condens. Matter 6 9211

(http://iopscience.iop.org/0953-8984/6/43/019)

J. Phys.: Condens. Matter 6 (1994) 9211–9218. Printed in the UK

Photoconductivity study of synthetic FeS_2 single crystals at low temperatures

S H Chen†, M Y Tsay†, Y S Huang†§ and J T Yu‡

† Department of Electronic Engineering, National Taiwan Institute of Technology, Taipei 106, Taiwan

‡ Institute of Physics, National Taiwan Normal University, Taipei 117, Taiwan

Received 10 March 1994, in final form 13 June 1994

Abstract. The photoconductivity measurements of synthetic pyrite FeS_2 single crystals at low temperatures are used to study the impurity and defect-related photoresponse peaks below the band edge. At temperatures below 100 K, several features on the low-energy side of the photoconductivity spectra are observed. By comparison of the results with those of the absorption and the photo-EPR measurements, the origin of the sharpest peak at 0.866 eV is identified. The nature of other weaker features is discussed. The existence of these features prevents us from determining the band gap of FeS_2 by the Moss rule at low temperature. We propose that the energy gap of FeS_2 at low temperatures may be determined by adding the thermal ionization energy of the shallow acceptor states to the photo-ionization energy between the $(SCl)^{2-}$ states and the bottom of the conduction band.

1. Introduction

Pyrite (FeS_2) has received growing attention in recent years owing to its potential application as a useful material for solar energy applications [1, 2], as a cathode in high-energy-density batteries [3, 4] and as a depolarizer anode for hydrogen production [5]. In natural samples the high impurity concentration disturbs its photoactive properties, so that synthetic material has to be fabricated. Electron paramagnetic resonance (EPR) investigations have revealed the unintentional Cr^{3+} and Ni^{2+} impurities and the $(SX)^{2-}$ (X ≡ Br or Cl) defects in chalcogen-deficient crystals [6–8]. The transport properties and the photoconductive spectral response of these synthetic FeS_2 crystals are thought to be controlled by these impurities and defects.

In our previous report, we presented the results of photoconductivity measurements of synthetic FeS_2 crystals [9]. The energy gap was determined from the photoconductive spectral response by the Moss [10] rule. The indirect energy gap was determined to be 0.83 ± 0.02 eV. The band gap was found to vary linearly with temperature between 100 and 300 K. However, no detailed analysis of the photoresponse features below the band edge was reported. Yang *et al* [11] recently made low-temperature IR absorption measurements of these same batches of crystals. They have observed several sharp peaks superimposed on the absorption curve at temperatures lower than about 150 K. The sharpest is located at 0.865 eV at 80 K. Yu *et al* [12] investigated the spectral response of the photoquenching of Cr^{3+} at 114 K and found that the response is the largest near 1.4 μm. In this paper, we extend our studies on the additional features below the absorption edge at temperatures

§ Author to whom correspondence should be addressed.

0953-8984/94/439211+08$19.50

lower than 150 K. By comparison of the results with that of the absorption and the photo-EPR measurements [12], the origin of the sharpest peak at 0.866 eV is identified. The nature of other weaker features is discussed. The existence of these features prevents us from analysing the band-gap nature of FeS_2 by the Moss [10] rule. Therefore a new approach to the determination of the energy gap at low temperatures is proposed and will be discussed in the later sections.

2. Experimental details

Single crystals of FeS_2 with mirror-like surfaces have been grown by an oscillating chemical vapour transport method [13]. The oscillating method allows large crystals to grow at the expense of small crystals and leads to a small number of larger single crystals. Prior to the crystal growth, a powdered compound was prepared from the elements Fe (purity 99.995%) and S (purity 99.9998%) by a reaction at 600 °C for 7 d in an evacuated quartz ampoule. To improve the stoichiometry, sulphur with 2 mol% in excess was added with respect to the stoichiometric mixture of the constituent elements. The mixture was slowly heated to 600 °C. The slow heating is necessary to avoid any explosions due to the strongly exothermic reaction between the elements. The lattice parameters were determined by x-ray powder diffraction analysis and the pyrite crystal structure was confirmed. The chemical transport was achieved with ICl_3 as a transport agent in the usual amount of 5 mg cm^{-3}. A reaction in the temperature gradient 700–580 °C during 21 d produced large single crystals up to 5 mm × 5 mm × 5 mm. The (100) face appears to be the predominant growth face. Trace element concentrations in the crystals were measured by inductively coupled plasma mass spectrometry. Cr and Ni were detected as unwanted impurities. It was reported [16] that the pyrite structure favours the enrichment of Cr and Ni during crystallization. This was explained by the high crystal-field stabilization energies of Cr and Ni in a strong octahedral ligand field, its strength being well documented by the low-spin states Fe^{2+} in pyrite. Electrical resistivity and Hall effect measurements have revealed p-type semiconducting behaviour. At room temperature, the carrier concentrations are between 6×10^{15} and 7×10^{16} cm^{-3}, and the mobilities between 50 and 200 cm^2 V s^{-1}. The measured values of the mobilities were very high for p-type pyrite. This might be due to a compensation effect induced by the presence of impurities and defects. The measured values varied considerably from sample to sample, and this was attributed to uncontrollable impurity concentration or non-stoichiometric effects.

The FeS_2 crystals used in this study include crystals obtained from two different growth runs: type A crystals from growth run A; type B crystals from growth run B. For type A crystals, a slightly larger than stoichiometric amount of sulphur (2 mol% in excess) was used in the starting materials for crystal growth. The sulphur content in type A crystals as determined by energy-dispersive x-ray spectroscopy (EDXS) is slightly deficient ($FeS_{1.91}$). The EPR spectrum of the $(SCl)^{2-}$ species is determined. Type B crystals are recrystallized crystals, but no extra sulphur was added in the initial and final crystal growth runs. These crystals exhibit a more significant deficiency in sulphur ($FeS_{1.85}$ by EDXS). The signal intensity of the EPR spectrum of the $(SCl)^{2-}$ species is about two orders of magnitude larger than that observed in growth run A.

The details of the present experimental set-up have been described previously [9]. Prior to photoconductivity measurements, the crystals were cut into thin slabs with a diamond saw parallel to the prominent face (100). The as-grown (100) faces were then etched in a solution of HNO_3, HF and CH_3COOH mixed in the ratios 2:1:1 by volume and rinsed with ethanol.

Ohmic contacts were made by soldering indium with gold which led to Au-evaporated electrodes on the sample. The electrodes of sample were covered with a black shield to avoid irradiation by the light beam. The light source was an Osram 100 W quartz–halogen lamp operated by a stabilized 12 V power supply. Incident light was provided by the output of a PTI 0.25 m scanning monochromator equipped with a 600 groove mm^{-1} grating. A long pass filter was used to eliminate second-order light. The sample was then mounted on the end of a cold finger, which is housed in a vacuum chamber. The monochromatic light was admitted through a quartz window on the side of the chamber. The temperatures were controlled with a heater wound close to the sample and monitored with a calibrated silicon diode sensor which was placed alongside the sample. The measurements were made at several temperatures between 25 and 150 K with a temperature stability of 0.5 K or better.

3. Results and discussion

Figure 1(a) shows the relative photoconductive spectral response of a type A sample crystal normalized with incident light intensity at 25, 50, 75, 100, 125 and 150 K. At lower temperatures, at least five features are observed on the low-energy side of the photoconductivity spectra. These features shift to lower energies and become less pronounced as the temperature of the sample becomes higher than 125 K. At temperatures below 100 K, the positions of these features remain unchanged. For comparison, the transmittance spectra at 80 K from [10] is shown in figure 1(b). The photoconductivity features and the absorption peaks show a one-to-one correspondence. Table 1 gives the positions of these features at different temperatures. In order to identify the origin of these features, a detailed comparison with the recent absorption [11] and EPR studies on the same batches were made [12, 14]. Yu *et al* [12] reported the results of a photo-EPR study on FeS_2 crystals from the same batch of type A samples. They found a decrease (photoquenching) in the EPR signal of Cr^{3+} and an increase (photo-induction) in the EPR signal of $(SCl)^{2-}$ at low temperatures. As shown in figure 2, the spectral response of the photoquenching of Cr^{3+} is largest near 0.87 eV at temperatures of about 110 K. This is correlated with the sharpest peak of the photoconductivity spectra and the 0.865 eV IR absorption peak observed at low temperatures [12]. The process mainly responsible for the photoquenching of Cr^{3+} $3d^3$ is regarded as the absorption of a photoelectron by Cr^{3+} and its conversion into Cr^{2+} $3d^4$:

$$Cr^{3+} + e^-_{photo} \rightarrow Cr^{2+}. \tag{1}$$

No measurable timelag was observed for the photoquenching of the Cr^{3+} signal, but it took several minutes for the signal to reach a new equilibrium value after the cessation of IR illumination. The temporal response of the signal recovery was non-exponential. The signal did not recover its original value before IR illumination. These phenomena indicated the presence of trapping centres. The photoconductivity results indicate that the following thermal ionization process takes place:

$$Cr^{2+} \rightarrow Cr^{3+} + e^-(CB). \tag{2}$$

This process is depicted in the band diagram as shown in figure 3. The 0.876 eV feature is assigned as the photoexcitation of electrons from the top of the valence band to the Cr^{2+} trapping centre. A detailed kinetic description of the photoquenching of Cr^{3+} also includes the capture of conduction electrons by the Cr^{3+} ions, i.e.

$$Cr^{3+} + e^-(CB) \rightarrow Cr^{2+} \tag{3}$$

Table 1. Energy positions of the impurities and defects related features for synthetic FeS_2 single crystals at different temperatures.

Growth-A sample						
T(K)	E_1(meV)	E_2(meV)	E_3(meV)	E_4(meV)	E_5(meV)	
20	866 ± 5	876 ± 5	904 ± 5	916 ± 8	960 ± 10	
50	866 ± 5	876 ± 5	904 ± 5	916 ± 8	960 ± 10	
75	866 ± 5	876 ± 5	904 ± 5	916 ± 8	960 ± 10	
80[a]	865 ± 5	876 ± 5	904 ± 5	916 ± 8	959 ± 10	
100	865 ± 5	874 ± 5	903 ± 5	915 ± 8	958 ± 10	
125	864 ± 5	—	901 ± 5	913 ± 8	956 ± 10	
150	862 ± 5	—	—	—	—	
Growth-B sample						
T(K)	E_1(meV)	E_2(meV)	E_3(meV)	E_4(meV)	E_5(meV)	E_6(meV)
25	865 ± 5	875 ± 5	904 ± 5	917 ± 8	958 ± 10	1040 ± 10
50	865 ± 5	875 ± 5	904 ± 5	917 ± 8	958 ± 10	1040 ± 10
75	865 ± 5	875 ± 5	904 ± 5	917 ± 8	958 ± 10	1040 ± 10
100	864 ± 5	874 ± 5	903 ± 5	916 ± 8	957 ± 10	—
125	863 ± 5	—	902 ± 5	914 ± 8	956 ± 10	—
150	862 ± 5	—	899 ± 5	912 ± 8	—	—

[a] From [10].

and the capture of free holes by the Cr^{2+} ions, i.e.

$$Cr^{2+} + h^+ \rightarrow Cr^{3+}. \tag{4}$$

Kou and Seehra [15] reported an optical absorption study of natural single crystals of iron pyrite. At temperatures lower than 110 K, three sharp peaks at 0.866, 0.905 and 0.917 eV were superposed on the absorption curves. These peaks were tentatively designated as transitions to excitonic levels. However, the results of the recent photo-EPR study of synthetic FeS_2 crystals [12] might rule out the possibility of this assignment.

The spin-$\frac{1}{2}$ paramagnetic axial symmetry $(SCl)^{2-}$ species were also observed by EPR in sulphur-deficient FeS_2 crystals (type A batch) at temperatures below about 200 K [12]. The EPR signal amplitude of this species does not vary with temperature. It has been postulated that, in the case of sulphur deficiency, the molecular ion consisting of a sulphur atom and a chlorine atom takes the place of the S_2^{2-} molecular ion in FeS_2 [7, 8]. It was further assumed that the S^{2-} of this molecular ion behaves as an electron donor, and the ionized donor becomes $(SCl)^{2-}$ paramagnetic species detected by EPR. An alternative description of the S^- species was used in discussing the transient and equilibrium behaviours of this species [12]. The electron configuration of S^- is $3s^23p^5$, which is regarded as consisting of a hole in the 3p subshell. The capture of a free hole by the S^{2-} defect results in S^-:

$$S^{2-} + h^+ \rightarrow S^-. \tag{5}$$

The EPR signal of $(SCl)^{2-}$ is photo-induction. At 108 K, an average increase of $6.7 \pm 0.7\%$ was observed for the EPR signal amplitude during IR illumination of photon energy less than E_g. After the cessation of IR illumination, the signal amplitude was reduced very slowly to a new equilibrium value which was larger than before IR illumination. The photo-induction of $(SCl)^{2-}$ was explained by the hole-capture process given in equation (5). IR illumination releases free holes which are captured by the S^{2-} defect and the S^{2-} defect behaves as a hole trap. Since the 0.96 eV kink become a huge hump for the type B samples which

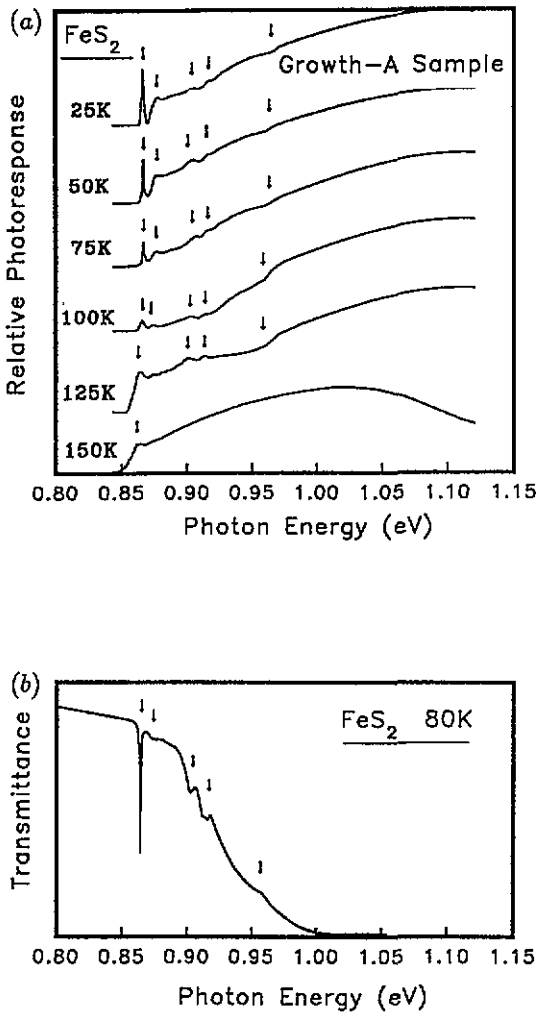

Figure 1. (a) The relative photoconductive spectral response for the type A sample crystal at 25, 50, 75, 100, 125 and 150 K. The energy positions of various features are indicated by arrows. (b) The transmittance spectra of the FeS_2 single crystal from the same batch of type A samples from [11].

exhibit significant sulphur deficiency (figure 4) and had not been observed in the natural sample crystals [15], the origin of this feature is tentatively assigned as the photo-ionization between the $(SCl)^{2-}$ impurity defect states and the bottom of the conduction band. The origin of the features at 0.904 and 0.916 eV remains undetermined. Further work is required to study the properties of these impurity- or defect-related trapping centres.

The relative photoconductive spectral response curve of a type B sample crystal at 50 K is shown in figure 4. Besides the features observed in the type A sample, an additional hump at around 1.04 eV is observed. This additional feature is very sensitive to the temperature and becomes noticeable at temperatures lower than 75 K. This could be explained by assuming that at high temperatures the acceptors are mainly ionized so that the rates of the photo-ionization are low. The possible origin of this feature will be discussed as follows.

Recently Wu *et al* [14] reported a new type of spin-$\frac{1}{2}$ chlorine-associated defect species

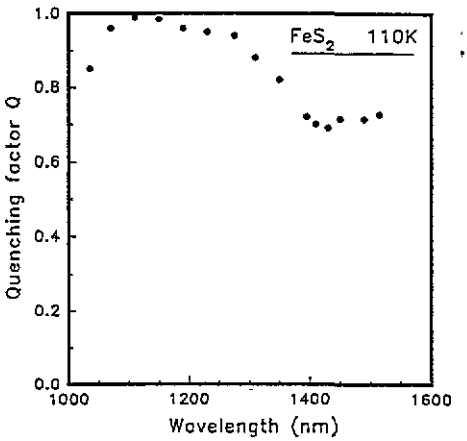

Figure 2. The spectral response of the photoquenching of Cr^{3+} at $T = 114$ K from [12]; the measured quenching factor Q is plotted as a function of the incident wavelength.

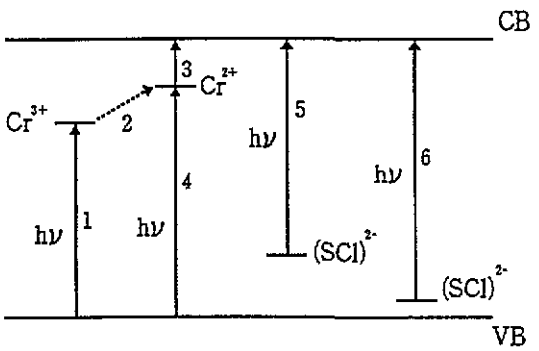

Figure 3. A schematic diagram depicting the photo-ionization and thermal ionization processes affecting the photoquenching of Cr^{3+}, and the photo-ionization processes related to $(SCl)^{2-}$ impurity defects. Process 1 is the photoexcitation of an electron from the valence band to the Cr^{3+} level; process 2 is the conversion of a Cr^{3+} into Cr^{2+}; process 3 is the thermal ionization of an electron from the Cr^{2+} level to the conduction band; process 4 is the photoexcitation of an electron from the valence band to the Cr^{2+} level; process 5 is the photoexcitation of an electron from the $(SCl)^{2-}$ defect states to the conduction band; process 6 is the photoexcitation of an electron from the occupied $(SCl)^{2-}$ shallow acceptor level to the conduction band.

in the same batch of the FeS_2 crystals which exhibit significant sulphur deficiency and consequently significant doping of the chlorine impurity. The EPR spectrum of this defect species exhibits a low symmetry and a weak hyperfine interaction with a single chlorine nucleus. The g-factor anisotropy indicates that this species is a hole species, having a p^5 electron configuration and localized at a sulphur atom. This defect species was assigned as an $(SCl)^{2-}$ impurity defect, replacing $(S–S)^{2-}$ and locally associated with an Fe^{2+} vacancy created to compensate for the substantial Cr^{3+} impurities. According to the results

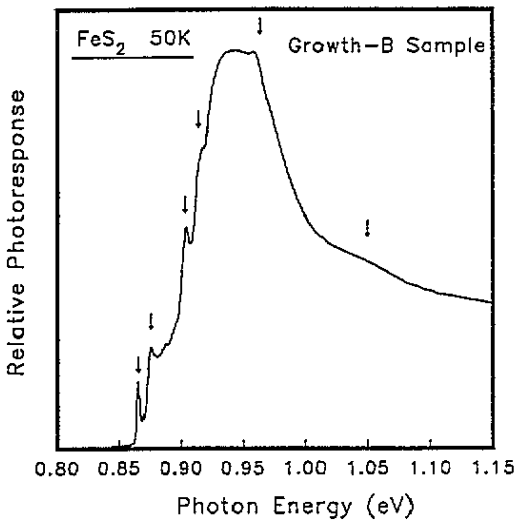

Figure 4. The relative photoconductive spectral response for the type B sample crystal at 50 K in the energy range 0.85–1.15 eV. The energy positions of various features are indicated by arrows.

of previous EPR study, we may assign the origin of the 1.04 eV feature as the photo-ionization transition between the non-axial $(SCl)^{2-}$ impurity defect states to the bottom of the conduction band, where the non-axial $(SCl)^{2-}$ defects form the shallow acceptor states. Further work is needed to understand the nature of these shallow acceptors.

In the previous reports there has been considerable controversy as to the value of the energy gap for FeS_2 [15, 16]. This might be because the methods used to analyse the experimental data are not appropriate. Most of the methods used to analyse the band-gap nature of FeS_2 assume that the electronic transitions are between two parabolic bands. However, this is not the case for FeS_2. From the results of the band-structure calculations by Bullett [17], it is known that the top of the valence band and the bottom of the conduction band are rather flat. In this study the existence of the features on the photoconductive spectra prevents us from determining the band gap of FeS_2 at low temperatures by the Moss [10] rule. We propose that one can estimate the energy gap of FeS_2 at low temperatures by adding the thermal ionization energy of the shallow acceptor states to the photo-ionization energy between the non-axial $(SCl)^{2-}$ impurity defect states and the bottom of the conduction band. The thermal ionization energy of the shallow acceptor states is estimated to be 50 ± 20 meV; then the energy gap below 75 K is determined to be 1.09 ± 0.03 eV.

4. Conclusion

Photoconductivity measurements of synthetic pyrite single crystals at low temperatures have been carried out. Several features below the band edge are observed. By comparison of the results with those of the absorption and the photo-EPR measurements, the origin of the sharpest peak at 0.866 eV is identified as the transition between the top of valence band and Cr^{3+} trapping centre. The origin of the 0.96 and 1.04 eV features are tentatively assigned as the photo-ionization between the $(SCl)^{2-}$ impurity defect states and the bottom of the conduction band. More systematic work is needed to establish conclusively the role

of impurities and defects in FeS_2. The band gap of FeS_2 below 75 K is estimated to be 1.09 ± 0.03 eV by adding the thermal ionization energy of the shallow acceptors to the photo-ionization energy between $(SCl)^{2-}$ states and the bottom of the conduction band.

Acknowledgments

The authors acknowledge the support of the National Science Council of the Republic of China.

References

[1] Jaegermann W and Tributsch H 1983 *J. Appl. Electrochem.* **13** 743
[2] Ennaoui A and Tributsch H 1984 *Solar Cells* **13** 197
[3] Vincent C A 1984 *Modern Batteries* (London: Edward Arnold) p 182
[4] Pemsler J M, Lam R K F, Litchfield J K, Dallek S, Larrick B F and Beard B C 1990 *J. Electrochem. Soc.* **137** 1
[5] Lalvani S B and Shami M 1986 *J. Electrochem. Soc.* **13** 1364
[6] Siebert D, Dahlem J, Fiechter S and Hartmann A 1989 *Z. Naturf.* a **44** 59
[7] Siebert D, Miller R, Fiechter S, Dulski P and Hartmann A 1990 *Z. Naturf.* a **45** 1267
[8] Yu J T, Wu C J, Huang Y S and Lin S S 1992 *J. Appl. Phys.* **71** 370
[9] Tsay M Y, Huang Y S and Chen Y F 1993 *J. Appl. Phys.* **74** 2786
[10] Moss T S 1959 *Photoconductivity in the Elements* (London: Butterworth)
[11] Yang J R, Yu J T, Huang J K, Tsay M Y and Huang Y S 1994 *to be published*
[12] Yu J T, Huang Y S and Tsay M Y 1994 *J. Appl. Phys.* **75** 5282
[13] Huang Y S and Lin S S 1988 *Mater. Res. Bull.* **23** 277
[14] Wu C J, Yu J T, Huang Y S and Lee C H 1994 *Japan. J. Appl. Phys.* **33** 2548
[15] Kou W W and Seehra M S 1978 *Phys. Rev.* B **18** 7062
[16] Ferrer I J, Nevskaia D M, de las Heras C and Sanchez C 1990 *Solid State Commun.* **74** 913
[17] Bullett D W 1982 *J. Phys. C: Solid State Phys.* **15** 6163